

Experiments on near-wall structure of three-dimensional boundary layers

By K. A. Flack¹ AND J. P. Johnston¹

1. Motivations

Investigations of three-dimensional turbulent boundary layers have shown basic differences between two- and three-dimensional flows. These differences can significantly impact the modeling of three-dimensional flows since many flow models are based on results from two-dimensional boundary layers. In many cases (Johnston (1976) and Driver & Johnston (1989)) the shear stress vector direction has been shown to lag relative to the direction of the mean velocity gradient as the cross-flow grows downstream. Coincidence of these vectors is necessary for a scalar eddy viscosity modeling assumption. A second effect is a reduction in magnitude of the shear stress and/or the shear stress to turbulence energy ratio, a_1 . This reduction has been observed in several experiments, for example Pontikos & Bradshaw (1985) and Anderson & Eaton (1988). Recent numerical simulations (Spalart (1989) and Moin, *et al.* (1990)) also indicate wall-layer structural differences between two- and three-dimensional boundary layers.

The mechanisms by which cross-flow affects the structure of the boundary layer may not be the same in all situations. Anderson and Eaton proposed that streamwise vortices of one sign in the inner layer are overwhelmed by a mean streamwise vorticity of the opposite sign associated with the part of the cross-flow velocity profile near the wall. A net loss of one-sign wall layer structures may reduce the active turbulence in the near-wall region and thereby reduce the Reynolds shear stresses across the boundary layer. Anderson and Eaton's hypothesis was indirectly verified in related experiments by Shizawa & Eaton (1990, 1992). Eaton (1991), in his interpretation of these data, shows that coherent, streamwise vortices of the same sign as the cross-flow vorticity in the wall-layers interact with the cross-flow to form an upwash of low momentum fluid from the wall: a flow similar to a longitudinal low-speed streak. Conversely, a vortex of the opposite sign interacts with the near-wall cross-flow quite differently. The upwash is suppressed so much that the formation of longitudinal low-speed streaks is prevented.

The reduction of shear stress and kinetic energy in the simulation of Sendstad & Moin (1991 a,b) appears to be related to the weakening and breakup of the near-wall high and low speed streaks as the streamwise vortices in the buffer layer, just above the streaks, are first shifted sideways (convected) by the cross-flow and then turned so they cut across the streaks at acute angles. However, the profile of mean streamwise vorticity (due to the cross-flow) for the simulated three-dimensional

¹ Stanford University

channel flow has only one sign, and it develops in a favorable pressure gradient, whereas almost all profiles seen in practice have a reversal of sign of streamwise vorticity somewhere in the buffer layer, and in many cases, they develop in adverse pressure gradients.

The differences in structure between two- and three-dimensional boundary layers was also addressed in the experiment of Littell & Eaton (1991). The experiment used two-point correlations to investigate the vortical structures in a three-dimensional boundary layer on a spinning disk. It was found that each sign of longitudinal vortex is equally likely to exist, but one sign of vorticity is associated with a structure which is better at producing ejections.

The goal of the current investigation is to study the structure of the inner layers. Among other questions, the differences between the effects deduced from the three-dimensional flow simulations and the effects seen in experiments can be examined. The research concentrates on the structure of the wall-layer through flow visualization and direct turbulence measurements down to $y^+ = 5$.

2. Accomplishments

2.1 Flow approaching a swept step

A three-dimensional boundary layer was produced by forcing the flow to turn rapidly ahead of a forward facing step which is swept back at 45° to the main flow. Strong boundary layer cross-flows are produced rapidly in response to severe spanwise pressure gradients imposed by the swept step; a case similar to an earlier investigation by Johnston (1970). The experiments are conducted in a low-speed water channel with $Re_\theta = 1400$ for the nominal two-dimensional boundary layer. The two-dimensional characteristics for the facility are already known from previous research (Barlow & Johnston, 1988, Johnson & Johnston, 1989).

2.1.1 Turbulence measurements

Turbulence measurements were obtained using a three-component LDA system at various locations upstream of the step. Profile locations ranged from an upstream station at $x' = 30.5$ cm to a station at $x' = 5.7$ cm, close to but downstream of the three-dimensional detachment line. The experimental configuration and measurement locations are diagrammed in Figure 1. Measurements of the turbulence intensity, shear stress magnitude, and structure parameter, a_1 , are shown on figures 2, 3, and 4 against y/δ and y^+ . These and other results are available in Flack & Johnston (1993).

The turbulence intensity grows downstream outside the wall region, and the location of peak intensity shifts away from the wall. The turbulent shear stress also grows downstream and reaches a maximum value in the neighborhood of $y^+ = 60$. The laminar portion of the total shear stress, shown in Figure 3(b), has the same contribution as the turbulent stress to the total stress at $y^+ = 10$.

The relative growth of the turbulent shear stress with respect to kinetic energy is represented in the structure parameter, a_1 , the ratio of the turbulent shear stress to twice the turbulent kinetic energy. a_1 decreased slightly downstream where cross-flows are large, but not as much as might be expected from examination of earlier

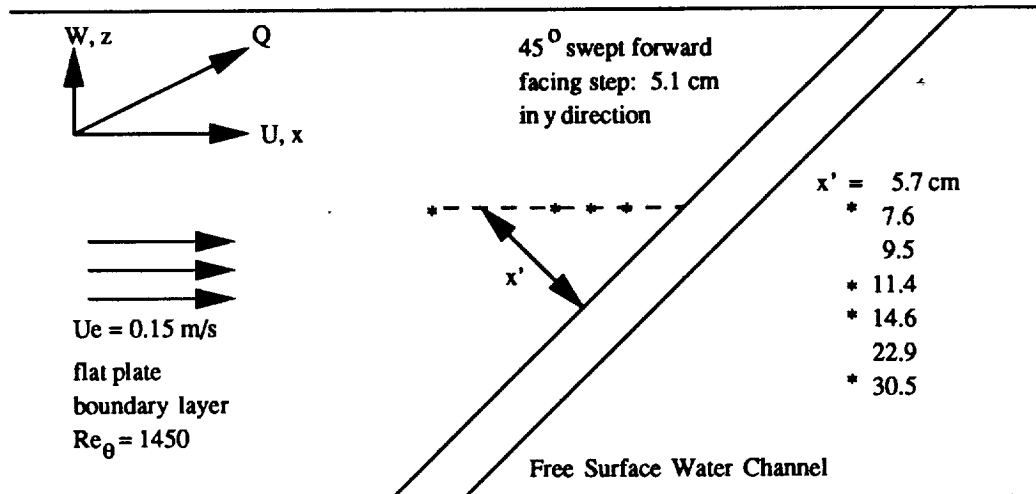


FIGURE 1. Experimental configuration: *, measurement locations presented.

studies such as the closely related flow of Johnston (1970). The effects of strong adverse pressure gradients, which occur in the same region as the strong cross-flows, may mask the effects of three-dimensionality on turbulence stress levels and thus on the a_1 parameter. It is interesting that a_1 seems to scale universally on y^+ up to $y^+ \approx 50$.

The response of the mean flow and turbulent shear stress to the onset of three-dimensionality is represented in the directions of the shear stress vector and the velocity gradient vector. These angles are shown in Figure 5 versus y/δ and y^+ . The shear stress is seen to lag the velocity gradient outside the sublayer region for $y^+ > 50$. Below $y^+ = 20$, it is hard to determine the relationship between angles because of high experimental uncertainty, but below y^+ of 30, the isotropic eddy viscosity assumption may be sufficient because the angles are nearly coincident.

2.1.2 Flow visualization

The near-wall flow structure was investigated through a series of flow visualization experiments. Three flow configurations were visualized for comparison: (1) a (base case) two-dimensional turbulent boundary layer, (2) a two-dimensional boundary layer flow approaching a forward facing step set perpendicular to the main flow, and (3) a three-dimensional boundary layer flow approaching the 45° swept, forward facing step. The hydrogen bubble wire technique was used to visualize the flow. Bubbles marked the flow at two locations; within the viscous sublayer at $y^+ \approx 2$ and within the buffer layer at $y^+ \approx 37$. The wall shear stress used in non-dimensionalization is based on the nominal two-dimensional boundary layer flow. The bubbles were illuminated in the cross-sectional view downstream of the wire using a laser light sheet and recorded on video tape for analysis.

The videos were viewed frame-by-frame to obtain "quantitative" results from the visualization. Vortical structures, a mass of hydrogen bubbles which appears

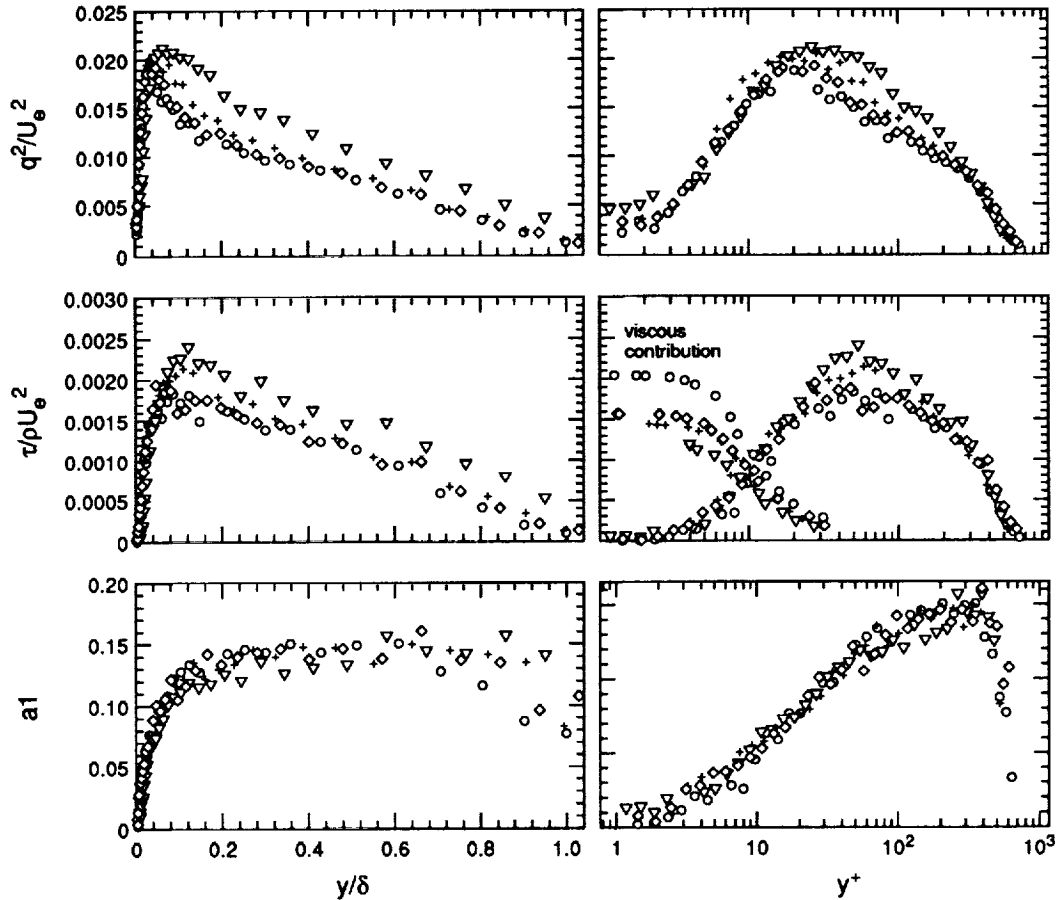


FIGURE 2. (a), (b): q^2/U_e^2 vs. y/δ and y^+ ; \circ , $x' = 30.5\text{cm}$; \diamond , $x' = 14.6\text{cm}$; $+$, $x' = 11.4\text{cm}$; ∇ , $x' = 7.6\text{cm}$.

FIGURE 3. (a), (b): $\tau/\rho U_e^2$ vs. y/δ and y^+ ; \circ , $x' = 30.5\text{cm}$; \diamond , $x' = 14.6\text{cm}$; $+$, $x' = 11.4\text{cm}$; ∇ , $x' = 7.6\text{cm}$.

FIGURE 4. (a), (b): a_1 vs. y/δ and y^+ ; \circ , $x' = 30.5\text{cm}$; \diamond , $x' = 14.6\text{cm}$; $+$, $x' = 11.4\text{cm}$; ∇ , $x' = 7.6\text{cm}$.

to be rotating or moving in a circular direction in the plane of the laser sheet, were identified and given a sign with relationship to the cross-flow. The size of the vortices (indicated by the normal extent of the bubble mass out from the wall beyond which bubbles could not be observed) was also recorded in viscous units. The vortical structures we observed are thought to represent cross-sections of the quasi-streamwise vortices observed by Robinson (1991).

Structural differences between the two- and three-dimensional boundary layers were observed by careful statistical analysis of at least 100 individual vortices for each case. It was found that both types of two-dimensional boundary layers, cases (1) and (2), contained equal numbers of each sign of vortex; however, for case (3), the

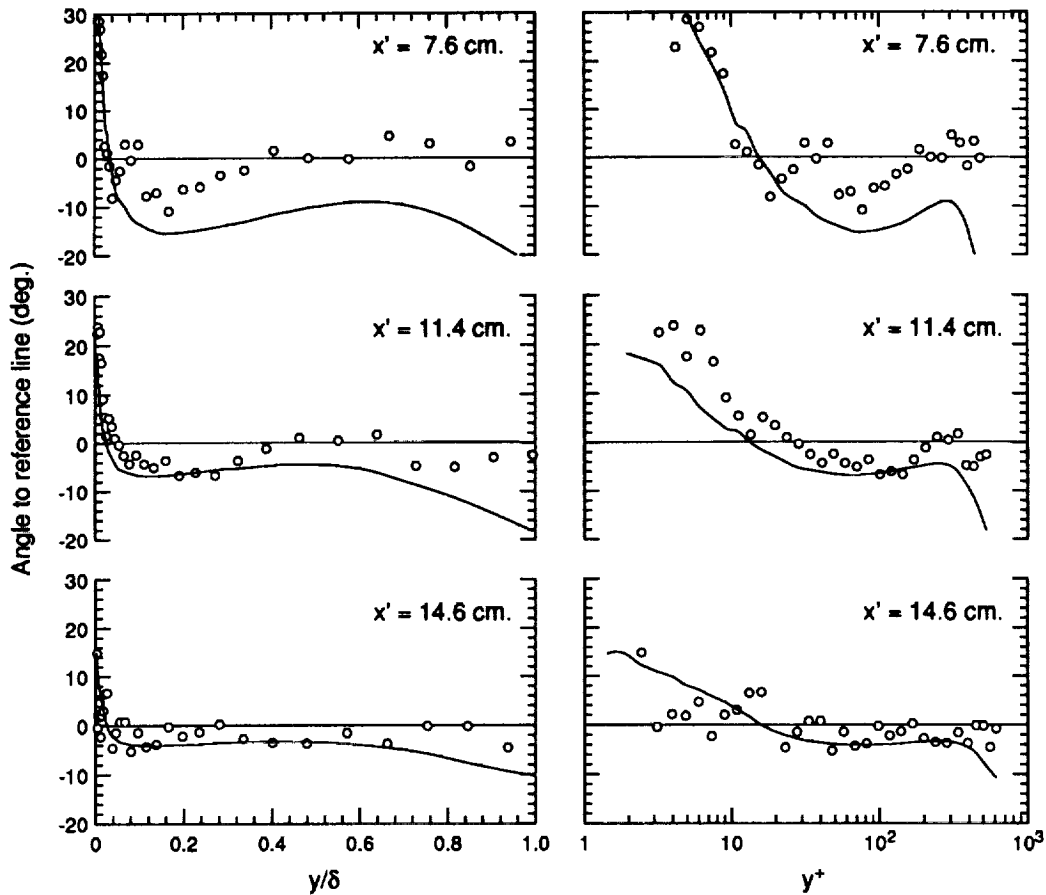


FIGURE 5. (a), (b): \circ , angles of shear stress; —, mean velocity gradient vs. y/δ and y^+ .

three-dimensional boundary layer at $y^+ = 37$ had excess (more than 50 %) vortices that have the same sign as the mean spanwise vorticity near the wall. This result can be interpreted in two ways with respect to previous findings. As hypothesized by Anderson & Eaton, there is a net loss of coherent wall layer structures of one sign which could be caused by the cancellation of vorticity by the mean vorticity near the wall. This preference for one sign of vortical structure could not be determined for the flow pictures marked at $y^+ = 2$, but it appeared in the picture at $y^+ = 37$ as noted.

This result can also be interpreted with respect to the findings of Littell & Eaton. Their research proposed that sweeps and ejections in the boundary layer were influenced by the mean vorticity associated with the cross-flow. Most strong ejections are caused by secondary velocity which augments the cross-flow close to the surface while most strong sweeps are caused by secondary velocity which opposes the cross-flow near the surface. In our visualization, the apparent increase in the number of

vortical structures with the same vorticity as the cross-flow near the surface could be due to a tendency in our visualization to identify the strong ejections as vortical structures.

The strong ejections caused by secondary velocity which augments the cross-flow close to the surface could also explain another finding from the flow visualization. From measurements of the vortex sizes, it was observed that vortices of both sign have the same average height and they reached out to the same maximum distance from the wall as seen in the two-dimensional boundary layers. However, in the three-dimensional case, the vortices with the same sign as the mean spanwise near-wall vorticity have a greater maximum and average height than the opposite signed vortices. Again, this could be the influence of the strong ejections.

2.2 Three-dimensional boundary layer facility

Preliminary turbulence measurements indicate that the abrupt swept-step flow shows some interesting features, but it is not typical of many important practical flows such as the three-dimensional boundary layer on the end wall of a bent duct or the flow over a swept wing. These cases are characterized by weaker streamwise and cross-flow pressure gradients, and, consequently, three-dimensionality in the boundary layer develops more slowly in the streamwise direction than is the case for swept-step flow. In order to study a slowly developing three-dimensional cross-flow on the flat wall of the channel, a new test section was recently constructed. This configuration consists of a 30° curved duct, similar to the flow investigated by Schwartz & Bradshaw (1992), whose experiment studied the outer regions of the boundary layer. The facility and instrumentation allow for measurements of velocity and turbulence profiles at selected streamwise stations along a curved arc representing the approximate path of the free-stream streamline in the region of small streamwise pressure gradients. Velocity measurements are obtained with a three component LDA system which obtains mean velocity vectors deep in the viscous region, $y^+ = 2$, and profiles of the six Reynolds stresses down to $y^+ = 5$. At the beginning of the duct curvature, the boundary layer is two-dimensional, has a $Re_\theta = 1250$, and is about 5.5 cm thick. Preliminary profiles indicate that the freestream turning is approximately 19° at the end of curvature and there is 36° of yaw.

3. Future plans

Our ongoing work will concentrate on the three-dimensional boundary layer for the curved duct flow. However, further investigation of the swept step case is also called for. Velocity profiles will be obtained for various stations along the centerline of the duct. Dye slots have been incorporated into the test section design to allow for visualization of the streaky structure in the near-wall region of the skewed flow. Hydrogen bubbles will also be employed to mark flow in the near wall region.

REFERENCES

- ANDERSON, S. D. & EATON, J. K. 1989 Reynolds stress development in a pressure

- driven three-dimensional turbulent boundary layer. *J. Fluid Mech.* **202**, 263-294.
- BARLOW, R. S. & JOHNSTON, J. P. 1988 Structure of a turbulent boundary layer on a concave surface. *J. Fluid Mech.* **191**, 137-176.
- BRADSHAW, P. & PONTIKOS, N. S. 1985 Measurements in the turbulent boundary layer on an 'infinite' swept wing. *J. Fluid Mech.* **159**, 105-130.
- DRIVER, D. M. & JOHNSTON, J. P. 1990 Experimental study of a shear-driven turbulent boundary layer flow with streamwise adverse pressure gradient. *Thermosciences Division, Stanford University, Stanford, CA, Report MD-57*.
- EATON, J. K. 1991 Turbulence structure and heat transfer in three-dimensional boundary layers. *9th Sympo. on Energy Engr, Sci., Argonne Nat. Lab.*
- JOHNSON, P. L. & JOHNSTON, J. P. 1989 The effects of grid-generated turbulence on flat and concave turbulent boundary layers. *Thermosciences Division, Stanford University, Stanford, CA, Report MD-59*.
- JOHNSTON, J. P. 1970 Measurements in a three-dimensional boundary layer induced by a swept, forward-facing step. *J. Fluid Mech.* **42**, 823-844.
- JOHNSTON, J. P. 1976 Experimental studies in three-dimensional turbulent boundary layers. *Thermosciences Division, Stanford University, Stanford, CA, Report MD-34*.
- FLACK, K. A. & JOHNSTON, J. P. 1993 Experimental study of a detaching three-dimensional boundary layer. *International Conference on Near-Wall Turbulent Flows, Tempe, AZ*.
- LITTELL, H. S. & EATON, J. K. 1991 An experimental investigation of the three-dimensional boundary layer on a rotating disk. *Thermosciences Division, Stanford University, Stanford, CA, Report MD-60*.
- MOIN, P., SHIH, T. H., DRIVER, D. M. & MANSOUR, N. N. 1990 Direct numerical simulation of a three-dimensional turbulent boundary layer. *Physics of Fluids*. **2**, 1846-1853.
- ROBINSON, S. K. 1991 Coherent motions in the turbulent boundary layer. *Annual Rev. Fluid Mech.* **23**, 601-639.
- SCHWARZ, W. R. & BRADSHAW, P. 1993 Measurements on a pressure-driven three-dimensional turbulent boundary layer during development and decay. *AIAA 31st Aerospace Sciences Meeting, Reno, NV, Paper 93-0543*.
- SENDSTAD, O. & MOIN, P. 1991 Numerical study of a three-dimensional boundary layer. *Workshop on Turbulence Structure and Control, AFOSR & Ohio State U., Columbus, OH*.
- SENDSTAD, O. & MOIN, P. 1991 On the mechanics of three-dimensional turbulent boundary layers. *8th Sympo. on Turbulent Shear Flows, Munich, Germany*.
- SHIZAWA, T. & EATON, J. K. 1990 Mean flow development of a longitudinal vortex embedded in an attached, three-dimensional turbulent boundary layer. *Intl. Sympo. on Engineering Turbulence Modelling and Measurements, Dubrovnik*.

- SHIZAWA, T. & EATON, J. K. 1992 Turbulence measurements for a longitudinal vortex interacting with a three-dimensional turbulent boundary layer. *AIAA J.* **30**, 1180-1181.
- SPALART, P. R. 1989 Theoretical and numerical study of a three-dimensional turbulent boundary layer. *J. Fluid Mech.* **205**, 319-340.